Atmos. Chem. Phys. Discuss., 12, 17583–17605, 2012
www.atmos-chem-phys-discuss.net/12/17583/2012/
doi:10.5194/acpd-12-17583-2012

Atmospheric Chemistry and Physics Discussions

The sensitivity of stratospheric ozone changes through the 21st century to N_2O and CH_4

L. E. Revell[1,2], G. E. Bodeker[3], P. E. Huck[3], B. E. Williamson[2], and E. Rozanov[4,5]

[1]National Institute of Water and Atmospheric Research, Christchurch, New Zealand
[2]Department of Chemistry, University of Canterbury, New Zealand
[3]Bodeker Scientific, Alexandra, New Zealand
[4]Physical-Meteorological Observatory Davos/World Radiation Center, Davos, Switzerland
[5]Institute for Atmospheric and Climate Science ETH, Zurich, Switzerland

Received: 11 June 2012 – Accepted: 28 June 2012 – Published: 18 July 2012

Correspondence to: L. E. Revell (laura.revell@niwa.co.nz)

Published by Copernicus Publications on behalf of the European Geosciences Union.

Abstract

Through the 21st century, anthropogenic emissions of the greenhouse gases N_2O and CH_4 are projected to increase, thus increasing their atmospheric concentrations. Consequently, reactive nitrogen species produced from N_2O and reactive hydrogen species produced from CH_4 are expected to play an increasingly important role in determining stratospheric ozone concentrations. Eight chemistry-climate model simulations were performed to assess the sensitivity of stratospheric ozone to different emissions scenarios for N_2O and CH_4. Increases in reactive nitrogen-mediated ozone loss resulting from increasing N_2O concentrations lead to a decrease in global-mean total column ozone. Increasing CH_4 concentrations increase the rate of reactive hydrogen-mediated ozone loss in the upper stratosphere. Overall however, increasing CH_4 concentrations lead to an increase in global-mean total column ozone. Stratospheric column ozone over the 21st century exhibits a near-linear response to changes in N_2O and CH_4 surface concentrations, which provides a simple parameterization for the ozone response to changes in these gases.

1 Introduction

Through the 21st century, declining concentrations of stratospheric chlorine and bromine, together with increasing concentrations of CO_2, are projected to lead to increased global-mean stratospheric ozone (Eyring et al., 2010). CO_2, the dominant anthropogenic greenhouse gas (GHG), elevates ozone by cooling the stratosphere, which slows the gas-phase ozone loss cycles (e.g. WMO, 1999; Rosenfield et al., 2002; IPCC/TEAP 2005). Of the GHGs controlled under the Kyoto Protocol, those with the highest radiative forcing after CO_2 are N_2O and CH_4, both of which lead to changes in ozone via chemical processes. Although the roles of N_2O and CH_4 in ozone chemistry are qualitatively understood, the sensitivity of ozone to these gases has not been

ACPD
12, 17583–17605, 2012

thoroughly investigated. It is the aim of this work to gain a quantitative understanding of the sensitivity of stratospheric ozone to N_2O and CH_4.

N_2O in the stratosphere affects ozone predominantly through NO_x-catalyzed ($NO_x = NO + NO_2$) ozone-loss cycles (Crutzen, 1970). However increases in N_2O do not necessarily lead to increases in NO_x, due to the interfering effects of other GHGs and ozone-depleting substances (ODSs). For example, the sink for NO_x is temperature dependent, so CO_2-induced cooling of the stratosphere decreases NO_x abundances (Rosenfield and Douglass, 1998). Plummer et al. (2010) found that nitrogen species incited large stratospheric ozone losses once the effects of CO_2-induced stratospheric cooling were removed. CH_4 weakens the ozone-depleting effectiveness of N_2O by producing reactive hydrogen species which: (1) slow NO_x-catalyzed ozone loss cycles in the upper stratosphere, and (2) remove NO_x from the middle stratosphere through reactions to form HNO_3 (Revell et al., 2012). Similarly, chlorine radicals produced by photolysis of ODSs such as the CFCs react with NO_x to form $ClONO_2$, thus reducing NO_x abundances (Ravishankara et al., 2009). However, as the chlorine loading of the stratosphere decreases through the 21st century (owing to the success of the Montreal Protocol for Substances that Deplete the Ozone Layer and later amendments), the effect of chlorine on NO_x will become less important. Furthermore, Ravishankara et al. (2009) have shown that N_2O is the dominant ODS currently emitted, and is expected to remain so through the remainder of the 21st century.

The oxidation of CH_4 produces HO_x radicals (here: $HO_x = H + OH + HO_2$), which catalyze ozone destruction cycles, particularly in the upper stratosphere. However, Portmann and Solomon (2007) and Fleming et al. (2011) have shown that the predominant effect of increasing CH_4 is to increase total column ozone by way of H_2O-induced stratospheric cooling in the middle stratosphere, which slows the temperature-dependent gas-phase ozone loss cycles. In addition, increasing CH_4 increases the reaction rate of Reaction (R1) (see below), which increases the rate of conversion of

ACPD
12, 17583–17605, 2012

chlorine to the HCl reservoir and thereby slows the chlorine-catalyzed ozone loss cycles throughout the stratosphere.

$$CH_4 + Cl \rightarrow CH_3 + HCl \quad \text{(R1)}$$

Furthermore, in the troposphere and very lower stratosphere, where the concentration of CO is sufficiently large (Lanzendorf et al., 2001), increased HO_x causes an increase in the rates of Reactions (R2)–(R5), therefore leading to ozone production (Brasseur and Solomon, 2005; Fleming et al., 2011). Likewise, increased NO_x (from elevated N_2O concentrations) leads to ozone production in the troposphere and lower stratosphere via Reactions (R4) and (R5).

$$OH + CO + O_2 \rightarrow HO_2 + CO_2 \quad \text{(R2)}$$

$$HO_2 + NO \rightarrow OH + NO_2 \quad \text{(R3)}$$

$$NO_2 + h\nu \rightarrow NO + O \quad \text{(R4)}$$

$$O + O_2 + M \rightarrow O_3 + M \quad \text{(R5)}$$

$$CO + 2O_2 \rightarrow CO_2 + O_3$$

Oman et al. (2010) studied the effects of reactive nitrogen and hydrogen species on stratospheric ozone using two chemistry-climate model (CCM) simulations constrained by the IPCC SRES A1B and A2 emissions scenarios for GHGs, which portray intermediate (A1B) and large (A2) increases in CO_2, N_2O and CH_4 (Nakicenovic and Swart, 2000). The evolution of upper stratospheric ozone in the two CCM simulations was similar, because although NO_x and HO_x species led to larger ozone losses in A2 compared with A1B, they were compensated by the effects of larger increases in CO_2-induced stratospheric cooling.

Here an analysis of the chemical sensitivity of stratospheric ozone to N_2O and CH_4 through the 21st century is presented using the results from eight CCM simulations. Four simulations differed only in terms of their N_2O concentrations, while the other four differed by their CH_4 concentrations. The same concentration scenario for CO_2 was used across all eight simulations.

ACPD
12, 17583–17605, 2012

2 Computational methods

2.1 The NIWA-SOCOL chemistry-climate model

The evolution of stratospheric ozone was simulated using the NIWA-SOCOL (National Institute of Water and Atmospheric Research – SOlar Climate Ozone Links) CCM (SPARC CCMVal, 2010). NIWA-SOCOL is based on SOCOL v2.0 (Schraner et al., 2008), which consists of the MAECHAM4 global climate model (Manzini et al., 1997) coupled to a modified version of the MEZON chemistry transport model (Egorova et al., 2003). NIWA-SOCOL includes 41 chemical species, 140 gas-phase reactions, 46 photolysis reactions and 16 heterogeneous reactions. Chemical constituents are advected by a hybrid transport scheme (Zubov et al., 1999), and the chemical solver algorithm uses a Newton-Raphson iterative method. A 15-min time step is used for dynamical processes, while radiative and chemical calculations are performed every two hours. CCM simulations were performed for the period 2005–2100, with the first ten yr discarded as spin-up.

The NIWA-SOCOL model attributes ozone loss to 15 catalytic cycles (listed in Revell et al., 2012), using a diagnostic approach similar to that employed by Lee et al. (2002). Odd oxygen ($O + O(^1D) + O_3$) removal rates (molecules cm^{-3} s^{-1}) are calculated within the model based on the rate-limiting steps of the corresponding reaction cycles, recorded and accumulated as daily means in each model grid cell.

2.2 Concentrations scenarios

Eight GHG concentration scenarios were constructed, as described in Table 1, using combinations of the IPCC SRES A1B concentrations scenario for GHGs (Nakicenovic and Swart, 2000), and the four representative concentration pathways (RCPs) 2.6, 4.5, 6.0 and 8.5, named according to the radiative forcings (in $W m^{-2}$) reached by 2100. The RCPs were developed for the climate modelling community to provide possible concentration trajectories for the main climate change forcing agents. They do not include

ACPD
12, 17583–17605, 2012

socio-economic, emission and climate projections (van Vuuren et al., 2011). Surface concentrations of N_2O and CH_4 for the individual scenarios are shown in Fig. 1. All simulations used the SRES A1B scenario for CO_2 and the adjusted A1 scenario for halocarbons (Daniel et al., 2007).

Sea-surface temperatures (SSTs) were prescribed under the SRES A1B scenario using output from the ECHAM5/MPIOM atmosphere-ocean general circulation model (AOGCM). To test whether they would have been different if they had been calculated from AOGCM simulations using the constructed GHG concentration scenarios (Table 1), SSTs for each of the eight scenarios were simulated using the simple climate model MAGICC6, which is designed to emulate AOGCMs (Meinshausen et al., 2011). Globally averaged annual-mean SSTs under the SRES A1B and the eight GHG concentrations scenarios are displayed in Fig. 2. SSTs exhibit a greater spread by 2100 in simulations employing different CH_4 scenarios, owing to the greater radiative forcing of CH_4 compared with N_2O. However, results do not significantly differ from the A1B simulation (at most, there is a difference of 0.5 K between the CH_4-8.5- and A1B-based SSTs in 2100). The conclusions drawn in this study are therefore not impacted by using A1B-based SSTs for all simulations.

3 Results and discussion

In all eight CCM simulations performed for this study, global-mean total column ozone increases through the 21st century. The amount of increase is listed as ΔO_3 in the rightmost column of Table 1. In general, this increase is caused by a combination of a slowing of the gas-phase ozone loss cycles due to stratospheric cooling (Rosenfield et al., 2002), and decreasing concentrations of stratospheric chlorine and bromine resulting from the phase-out of halogenated ODSs under the Montreal Protocol (Bekki et al., 2011). The simulations with larger N_2O surface concentrations lead to a smaller increase in ozone (4.3 DU in N_2O-8.5 compared with 10 DU in N_2O-2.6), while those

ACPD
12, 17583–17605, 2012

with larger CH_4 surface concentrations lead to a larger increase in ozone (16.7 DU in CH_4-8.5 compared with 4.4 DU in CH_4-2.6).

To examine changes in chemically-induced ozone destruction, the differences in the global-mean rates of the nitrogen, hydrogen and chlorine cycles in the 2090s decade between (a) the N_2O-8.5 and N_2O-2.6 simulations and (b) the CH_4-8.5 and CH_4-2.6 simulations are shown in Fig. 3. The ozone-depleting nitrogen cycles speed up with increased N_2O throughout the upper and middle stratosphere, but remain largely unchanged in the lower stratosphere where concentrations of odd oxygen are diminished (Fig. 3a). Figure 3b shows that the ozone-depleting hydrogen cycles speed up with increased CH_4, particularly in the upper stratosphere. The chlorine cycles slow, due to an increase in the rate of Reaction (R1).

Figure 4a shows the difference between 2090s ozone in the N_2O-8.5 and N_2O-2.6 simulations as a function of latitude and pressure. Ozone is suppressed by as much as ~5–10 % in the middle stratosphere in the N_2O-8.5 simulation compared to the N_2O-2.6 simulation but is elevated by ~5 % in the tropical lower stratosphere (~100–70 hPa). The smaller ozone increase in the N_2O-8.5 simulation is expected and due to enhanced rates of the ozone-depleting nitrogen cycles. The elevated values in the tropical lower stratosphere are due to ozone production via Reactions (R4) and (R5). The difference between 2090s total column ozone in the N_2O-8.5 and N_2O-2.6 simulations is shown in Fig. 4b as a function of latitude. Because the middle stratosphere dominates the ozone column, total column ozone is decreased at all latitudes in the N_2O-8.5 simulation relative to the N_2O-2.6 simulation (but less so in the tropical stratosphere).

Figure 5 is similar to Fig. 4, but shows the differences between simulations CH_4-8.5 and CH_4-2.6. In simulation CH_4-8.5, ozone increases of up to ~15 % greater than those in the CH_4-2.6 simulation are seen throughout the stratosphere, except for in the upper stratosphere where ozone is suppressed by more than 5 % due to enhanced rates of the hydrogen ozone loss cycles. The increase in ozone in the middle and lower stratosphere can be attributed to an increase in the rate of Reaction (R1) slowing the chlorine ozone loss cycles, an increase in the rate of Reactions (R2)–(R5) due

ACPD
12, 17583–17605, 2012

to increased HO_x in the lower stratosphere (leading to increased ozone production), and a slowing of the nitrogen ozone loss cycles at ~15 hPa (Fig. 3b). Figure 5b shows that 2090s total column ozone exhibits a greater increase in all latitudes in simulation CH_4-8.5 compared with simulation CH_4-2.6, particularly in the Arctic.

To test whether there is a linear relationship between stratospheric ozone at the end of the 21st century, and the N_2O or CH_4 concentration at that time, linear fits to 2090s-mean stratospheric ozone columns (1–100 hPa) as a function of N_2O or CH_4 concentrations were calculated in five regions of the stratosphere (Figs. 6 and 7). The slopes for the linear fits in Figs. 6 and 7 are given in Table 2, along with the R^2 values. The shaded regions in Figs. 6 and 7 represent the 95 % confidence interval calculated for the slope and intercept of the linear regression models.

As shown in Fig. 6 and Table 2, the slopes for the linear fits are negative in all regions of the stratosphere, and the R^2 values exceed 0.94 everywhere. All fits are statistically significant from zero at the 95 % confidence level, indicating a strong linear relationship between stratospheric ozone abundance and N_2O concentrations. The linear fits between ozone and CH_4 in Fig. 7 all have positive slopes, and are statistically significantly different from zero at the 95 % confidence level in all regions of the stratosphere except for the Antarctic, where the R^2 value is 0.87. Elsewhere, the R^2 value exceeds 0.91. For both the N_2O and CH_4 simulations, sensitivities in the polar regions are enhanced compared with the tropics and midlatitudes.

Figures 8 and 9 show the slopes of linear fits to 2090s-ozone vs. N_2O or CH_4 surface concentrations as a function of pressure and latitude. Regions where the slope is not statistically significantly different from zero at the 95 % confidence bounds are hatched. Figure 8 shows that in the polar regions and throughout most of the middle stratosphere, ozone demonstrates a statistically significant negative linear relationship with N_2O. There is a positive correlation in the tropical lower stratosphere, where enhanced N_2O leads to ozone production. Figure 9 shows that ozone decreases linearly with increasing CH_4 in the upper stratosphere, and that this relationship is statistically significant at the 95 % confidence level. Statistically significant relationships between

ACPD
12, 17583–17605, 2012

ozone and CH_4 are also found, for example, through much of the tropical, northern-midlatitude and Arctic stratosphere, where ozone increases with increasing CH_4.

These linear relationships between ozone and N_2O and CH_4 over the range of RCP scenarios tested here suggest that perturbations to either stratospheric column ozone (using the results presented in Figs. 6 and 7) or to vertically resolved ozone (using the results presented in Figs. 8 and 9) can be incorporated into simple models of stratospheric ozone to capture the changes in ozone resulting from changes in N_2O and CH_4.

4 Conclusions

Total column ozone increases through the 21st century in all eight CCM simulations presented here. Larger increases are observed in simulations with low N_2O or high CH_4 concentrations. N_2O decreases stratospheric ozone abundance by increasing the rate of the ozone-depleting nitrogen cycles. Although mid- and lower-stratospheric ozone increase in response to increased CH_4, upper stratospheric ozone decreases due to an increase in the rate of the ozone-depleting hydrogen cycles. Furthermore, we have shown that at the end of the 21st century, stratospheric column ozone decreases linearly with increasing surface N_2O concentrations in all regions of the stratosphere. In contrast, stratospheric column ozone increases linearly with increasing CH_4 concentrations, however this relationship is not statistically significant at the 95 % confidence level in the Antarctic stratosphere. We have also shown the vertically-resolved relationship between ozone and N_2O and CH_4. Our conclusions are derived from simulations based on a single CO_2 concentration scenario, and ozone may not exhibit this linear sensitivity under different CO_2 scenarios; this will be the subject of future work.

Acknowledgements. We would like to thank Dan Smale for his help in running the NIWA-SOCOL simulations, and Malte Meinshausen for providing us with the MAGICC6 model.

ACPD
12, 17583–17605, 2012

References

Bekki, S., Bodeker, G. E., Bais, A. F., Butchart, N., Eyring, V., Fahey, D. W., Kinnison, D. E., Langematz, U., Mayer, B., Portmann, R. W., Rozanov, E., Braesicke, P., Charlton-Perez, A. J., Chubarova, N. E., Cionni, I., Diaz, S. B., Gillett, N. P., Giorgetta, M. A., Komala, N., Lefèvre, F., McLandress, C., Perlwitz, J., Peter, T., and Shibata, K.: Future ozone and its impact on surface UV, in: Scientific Assessment of Ozone Depletion: 2010, Global Ozone Research and Monitoring Project – Report No. 52, chapter 3, 516 pp., World Meteorological Organization, Geneva, Switzerland, 2011.

Brasseur, G. and Solomon, S.: Aeronomy of the Middle Atmosphere, 3rd Edn., Dordrecht, The Netherlands, 644 pp., 2005.

Crutzen, P. J.: The influence of nitrogen oxides on the atmospheric ozone content, Q. J. Roy. Meteor. Soc., 96, 320–325, 1970.

Daniel, J. S., Velders, G. J. M., Douglass, A. R., Forster, P. M. D., Hauglustaine, D. A., Isaksen, I. S. A., Kuijpers, L. J. M., McCulloch, A., and Wallington, T. J.: Halocarbon scenarios, ozone depletion potentials, and global warming potentials, in: Scientific Assessment of Ozone Depletion: 2006, Global Ozone Research and Monitoring Project–Report No. 50, chapter 8, 572 pp., World Meteorological Organization, Geneva, Switzerland, 2007.

Egorova, T. A., Rozanov, E. V., Zubov, V. A., and Karol, I. L.: Model for investigating ozone trends (MEZON), Izv. Atmos. Ocean. Phys., 39, 277–292, 2003.

Eyring, V., Cionni, I., Bodeker, G. E., Charlton-Perez, A. J., Kinnison, D. E., Scinocca, J. F., Waugh, D. W., Akiyoshi, H., Bekki, S., Chipperfield, M. P., Dameris, M., Dhomse, S., Frith, S. M., Garny, H., Gettelman, A., Kubin, A., Langematz, U., Mancini, E., Marchand, M., Nakamura, T., Oman, L. D., Pawson, S., Pitari, G., Plummer, D. A., Rozanov, E., Shepherd, T. G., Shibata, K., Tian, W., Braesicke, P., Hardiman, S. C., Lamarque, J. F., Morgenstern, O., Pyle, J. A., Smale, D., and Yamashita, Y.: Multi-model assessment of stratospheric ozone return dates and ozone recovery in CCMVal-2 models, Atmos. Chem. Phys., 10, 9451–9472, doi:10.5194/acp-10-9451-2010, 2010.

Fleming, E. L., Jackman, C. H., Stolarski, R. S., and Douglass, A. R.: A model study of the impact of source gas changes on the stratosphere for 1850–2100, Atmos. Chem. Phys., 11, 8515–8541, doi:10.5194/acp-11-8515-2011, 2011.

IPCC/TEAP, Metz, B., Kuijpers, L., Solomon, S., Andersen, S. O., Davidson, O., Pons, J., de Jager, D., Kestin, T., Manning, M., and Meyer, L.: Safeguarding the Ozone Layer and the

ACPD
12, 17583–17605, 2012

Global Climate System: Issues Related to Hydrofluorocarbons and Perfluorocarbons, Cambridge University Press, UK, Geneva, 2005.
Lanzendorf, E. J., Hanisco, T. F., Wennberg, P. O., Cohen, R. C., Stimpfle, R. M., Anderson, J. G., Gao, R. S., Margitan, J. J., and Bui, T. P.: Establishing the dependence of $[HO_2]/[OH]$ on temperature, halogen loading, O_3, and NO_x based on in situ measurements from the NASA-ER2, J. Phys. Chem. A, 105, 1535–1542, 2001.
Lee, A. M., Jones, R. L., Kilbane-Dawe, I., and Pyle, J. A.: Diagnosing ozone loss in the extratropical lower stratosphere, J. Geophys. Res., 107, D114110, doi:10.1029/2001JD000538, 2002.
Manzini, E., McFarlane, N. A., and McLandress, C.: Impact of the Doppler spread parameterization on the simulation of the middle atmosphere circulation using the MA/ECHAM4 general circulation model, J. Geophys. Res., 102, 25751–25762, 1997.
Meinshausen, M., Raper, S. C. B., and Wigley, T. M. L.: Emulating coupled atmosphere-ocean and carbon cycle models with a simpler model, MAGICC6 – Part 1: Model description and calibration, Atmos. Chem. Phys., 11, 1417–1456, doi:10.5194/acp-11-1417-2011, 2011.
Nakicenovic, N. and Swart, R. (eds.): IPCC Special Report on Emissions Scenarios, Cambridge University Press, Cambridge, UK, 2000.
Oman, L. D., Waugh, D. W., Kawa, S. R., Stolarski, R. S., Douglass, A. R. and Newman, P. A.: Mechanisms and feedback causing changes in upper stratospheric ozone in the 21st century, J. Geophys. Res., 115, D05303, doi:10.1029/2009JD012397, 2010.
Plummer, D. A., Scinocca, J. F., Shepherd, T. G., Reader, M. C., and Jonsson, A. I.: Quantifying the contributions to stratospheric ozone changes from ozone depleting substances and greenhouse gases, Atmos. Chem. Phys., 10, 8803–8820, doi:10.5194/acp-10-8803-2010, 2010.
Portmann, R. W. and Solomon, S.: Indirect radiative forcing of the ozone layer during the 21st century, Geophys. Res. Lett., 34, L02813, doi:10.1029/2006GL028252, 2007.
Ravishankara, A. R., Daniel, J. S., and Portmann, R. W.: Nitrous oxide (N_2O): the dominant ozone-depleting substance emitted in the 21st century, Science, 326, 123–125, doi:10.1126/science.1176985, 2009.
Revell, L. E., Bodeker, G. E., Smale, D., Lehmann, R., Huck, P. E., Williamson, B. E., Rozanov, E., and Struthers, H.: The effectiveness of N_2O in depleting stratospheric ozone, Geophys. Res. Lett., doi:10.1029/2012GL052143, in press, 2012.

ACPD
12, 17583–17605, 2012

Rosenfield, J. E. and Douglass, A. R.: Doubled CO_2 effects on NO_y in a coupled 2D model, Geophys. Res. Lett., 25, 4381–4384, 1998.

Rosenfield, J. E., Douglass, A. R., and Considine, D. B.: The impact of increasing carbon dioxide on ozone recovery, J. Geophys. Res., 107, D64049, doi:10.1029/2001JD000824, 2002.

Schraner, M., Rozanov, E., Schnadt Poberaj, C., Kenzelmann, P., Fischer, A. M., Zubov, V., Luo, B. P., Hoyle, C. R., Egorova, T., Fueglistaler, S., Brönnimann, S., Schmutz, W., and Peter, T.: Technical Note: Chemistry-climate model SOCOL: version 2.0 with improved transport and chemistry/microphysics schemes, Atmos. Chem. Phys., 8, 5957–5974, doi:10.5194/acp-8-5957-2008, 2008.

SPARC CCMVal: SPARC Report on the Evaluation of Chemistry-Climate Models, edited by: Eyring, V., Shepherd, T. G., and Waugh, D. W., SPARC Report No. 5, WCRP-132, WMO/TD-No. 1526, available at: http://www.atmosp.physics.utoronto.ca/SPARC, 2010.

van Vuuren, D. P., Edmonds, J., Kainuma, M., Riahi, K., Thomson, A., Hibbard, K., Hurtt, G. C., Kram, T., Krey, V., Lamarque, J. F., Masui, T., Meinshausen, M., Nakicenovic, N., Smith, S. J., and Rose, S. K.: The representative concentration pathways: an overview, Climatic Change, 109, 5–31, doi:10.1007/s10584-011-0148-z, 2011.

World Meteorological Organization: Scientific Assessment of Ozone Depletion: 1998, WMO Global Ozone Research and Monitoring Project – Report No. 44, Geneva, 1998.

Zubov, V., Rozanov, E., and Schlesinger, M.: Hybrid scheme for three-dimensional advective transport, Mon. Weather Rev., 127, 1335–1346, 1999.

ACPD

12, 17583–17605, 2012

Table 1. Summary of scenarios for the CCM simulations[a].

Simulation	N_2O scenario	CH_4 scenario	ΔO_3 (DU)[b]
N_2O-2.6	RCP 2.6	SRES A1B	10.0
N_2O-4.5	RCP 4.5	SRES A1B	7.6
N_2O-6.0	RCP 6.0	SRES A1B	4.9
N_2O-8.5	RCP 8.5	SRES A1B	4.3
CH_4-2.6	SRES A1B	RCP 2.6	4.4
CH_4-4.5	SRES A1B	RCP 4.5	5.2
CH_4-6.0	SRES A1B	RCP 6.0	9.1
CH_4-8.5	SRES A1B	RCP 8.5	16.7

[a] All simulations used the IPCC SRES A1B scenario for CO_2 and adjusted A1 scenario for halocarbons;
[b] Change in global-mean total column ozone through the 21st century (2090s decade minus the decade from 2015–2024), expressed in Dobson units.

ACPD
12, 17583–17605, 2012

Table 2. Linear regression model slopes and R^2 values.

		N_2O simulations		CH_4 simulations	
		Slope (DU ppb^{-1})	R^2 value	Slope (DU ppb^{-1})	R^2 value
Arctic	(63–90° N)	−10.4	0.942	7.9	0.995
Northern midlatitudes	(30–60° N)	−7.1	0.996	3.9	0.993
Tropics	(25° N–25° S)	−3	0.988	1.7	0.912
Southern midlatitudes	(30–60° S)	−6.7	0.995	2.7	0.976
Antarctic	(63–90° S)	−13.3	0.999	6.7	0.870

ACPD
12, 17583–17605, 2012

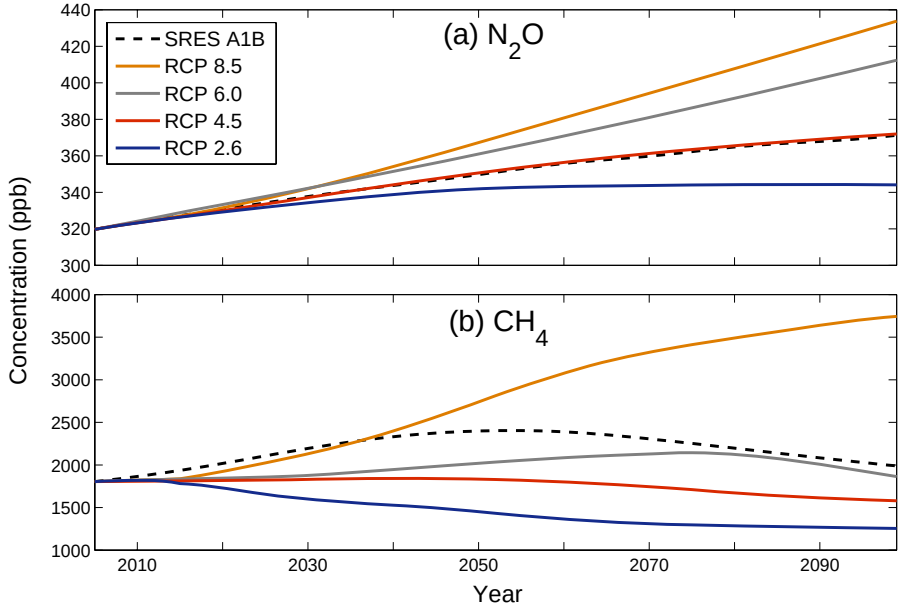

Fig. 1. (a) N_2O and **(b)** CH_4 surface concentrations used in the CCM simulations.

ACPD
12, 17583–17605, 2012

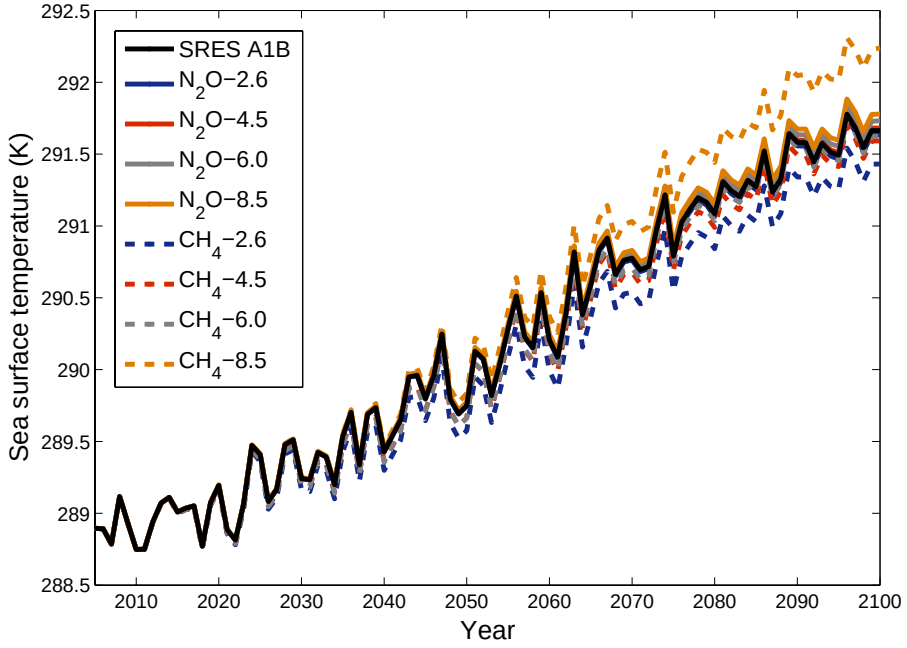

Fig. 2. Global-, annual-mean SSTs. The SRES A1B SSTs were used in all eight CCM simulations. The other SST series were calculated individually for each GHG concentration scenario using MAGICC6.

ACPD
12, 17583–17605, 2012

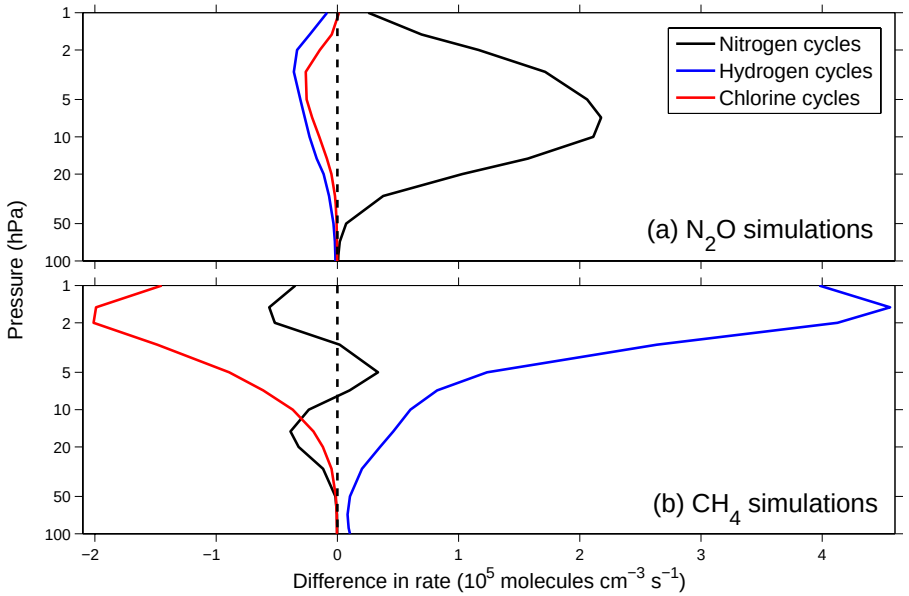

Fig. 3. (a) Global-mean contribution to ozone loss from the nitrogen, hydrogen and chlorine catalytic cycles in the 2090s decade in the N_2O-8.5 simulation, minus the same quantities for the N_2O-2.6 simulation. **(b)** Global-mean contribution to ozone loss from catalytic cycles in the 2090s decade in the CH_4-8.5 simulation, minus the same quantities for the CH_4-2.6 simulation.

ACPD
12, 17583–17605, 2012

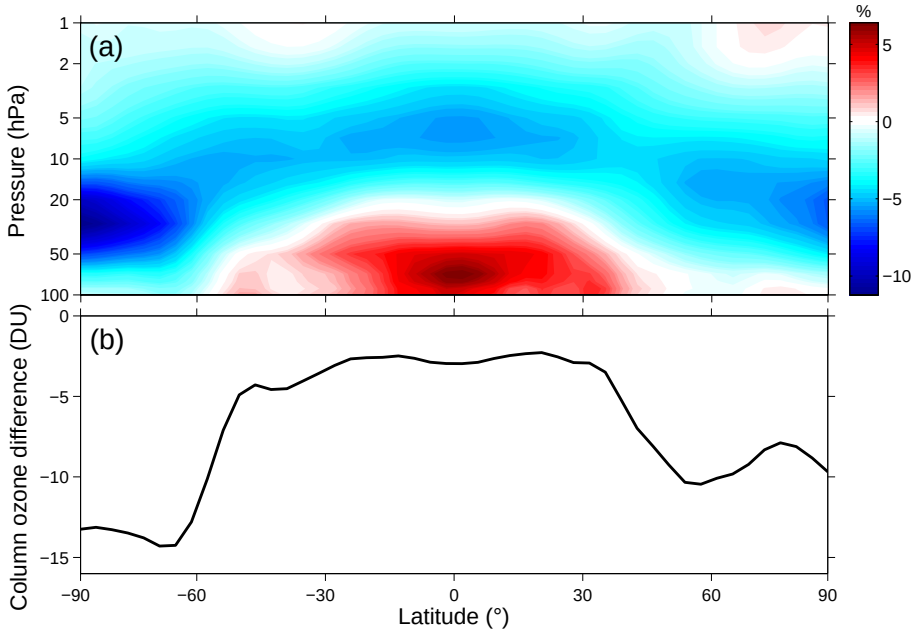

Fig. 4. (a) N_2O-8.5 ozone minus N_2O-2.6 ozone in the 2090s decade, calculated as a percentage of ozone in the N_2O-2.6 simulation. **(b)** 2090s-decade N_2O-8.5 total column ozone minus N_2O-2.6 total column ozone.

ACPD
12, 17583–17605, 2012

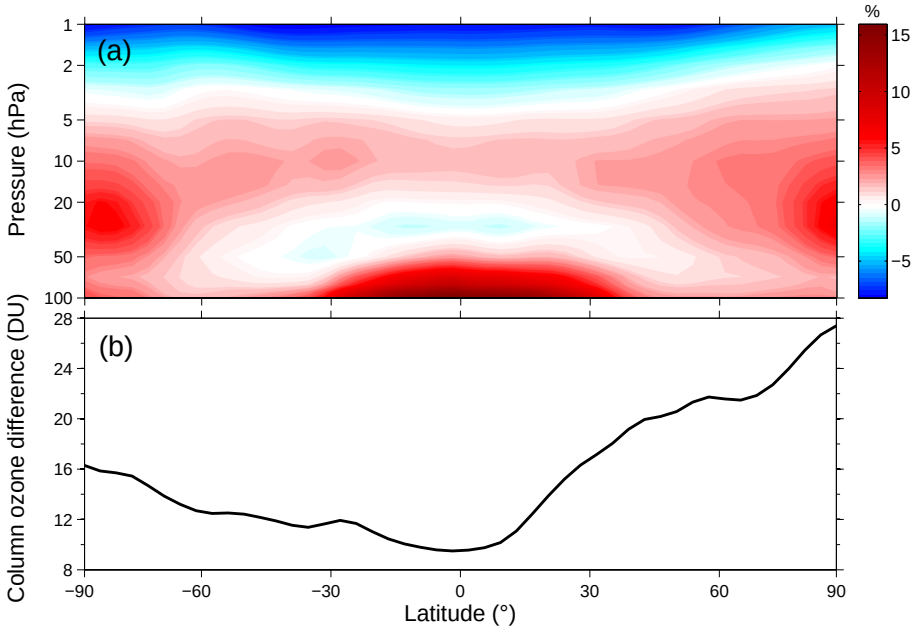

Fig. 5. (a) CH_4-8.5 ozone minus CH_4-2.6 ozone in the 2090s decade, calculated as a percentage of ozone in the CH_4-2.6 simulation. **(b)** 2090s-decade CH_4-8.5 total column ozone minus CH_4-2.6 total column ozone.

ACPD
12, 17583–17605, 2012

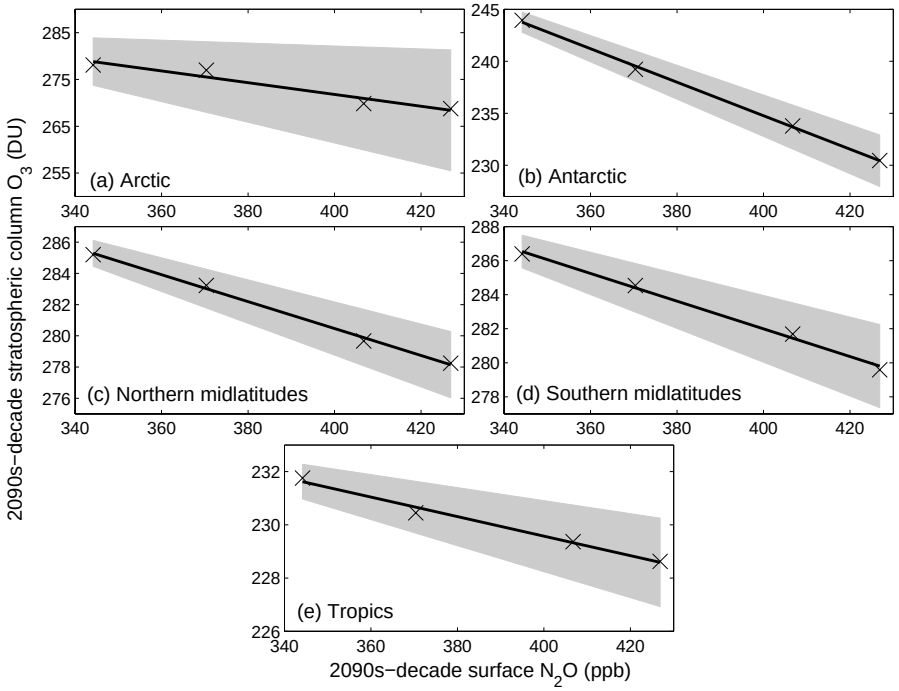

Fig. 6. (a) 2090s-mean Arctic (63–90° N) stratospheric column ozone (1–100 hPa) vs. 2090s-mean surface N_2O for the four N_2O simulations (crosses), fitted with a simple linear regression model (black line). The grey shaded region indicates the 95 % confidence interval for the slope and intercept of the regression model. **(b–e)** As for **(a)**, but for: **(b)** the Antarctic (63–90° S); **(c)** northern midlatitudes (30–60° N); **(d)** southern midlatitudes (30–60° S); **(e)** the tropics (25° N–25° S).

ACPD
12, 17583–17605, 2012

The sensitivity of stratospheric ozone changes

L. E. Revell et al.

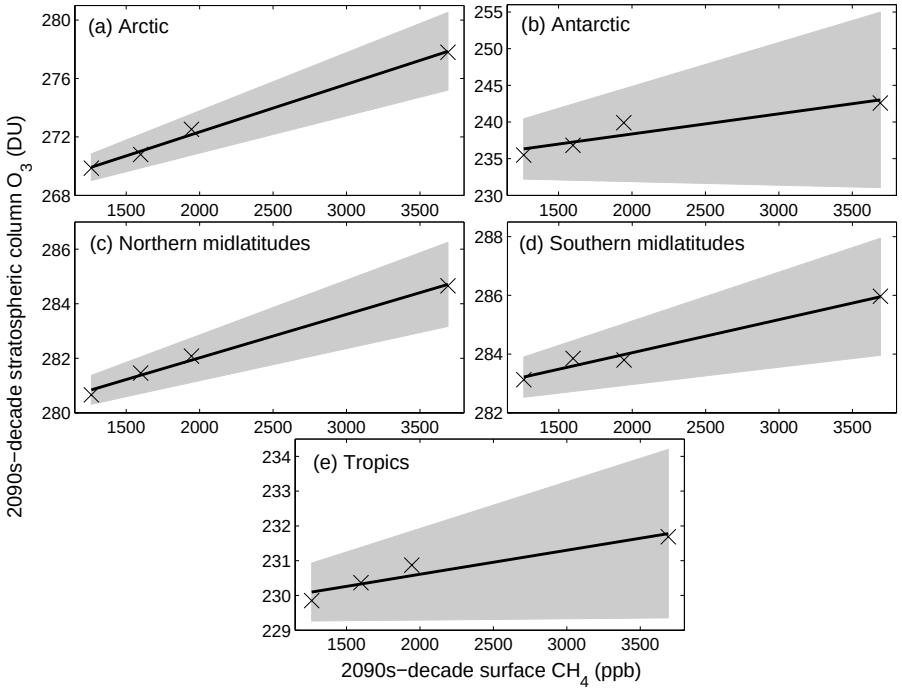

Fig. 7. Similar to Fig. 6, but for 2090s-mean stratospheric column ozone vs. 2090s-mean surface CH_4 for the four CH_4 simulations.

ACPD
12, 17583–17605, 2012

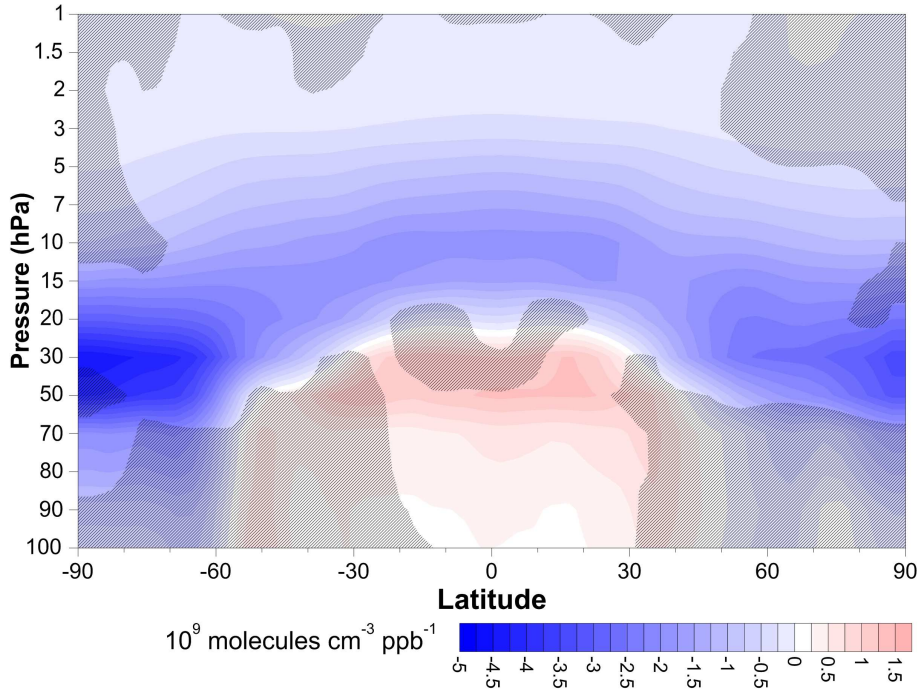

Fig. 8. Slopes from simple linear regression models fitted to 2090s-mean ozone vs. 2090s-mean surface N_2O for all latitudes and all pressure levels between 1–100 hPa, for the four N_2O simulations. Hatching indicates that the slope was not statistically significantly different from zero at the 95 % level of confidence.

ACPD
12, 17583–17605, 2012

The sensitivity of stratospheric ozone changes

L. E. Revell et al.

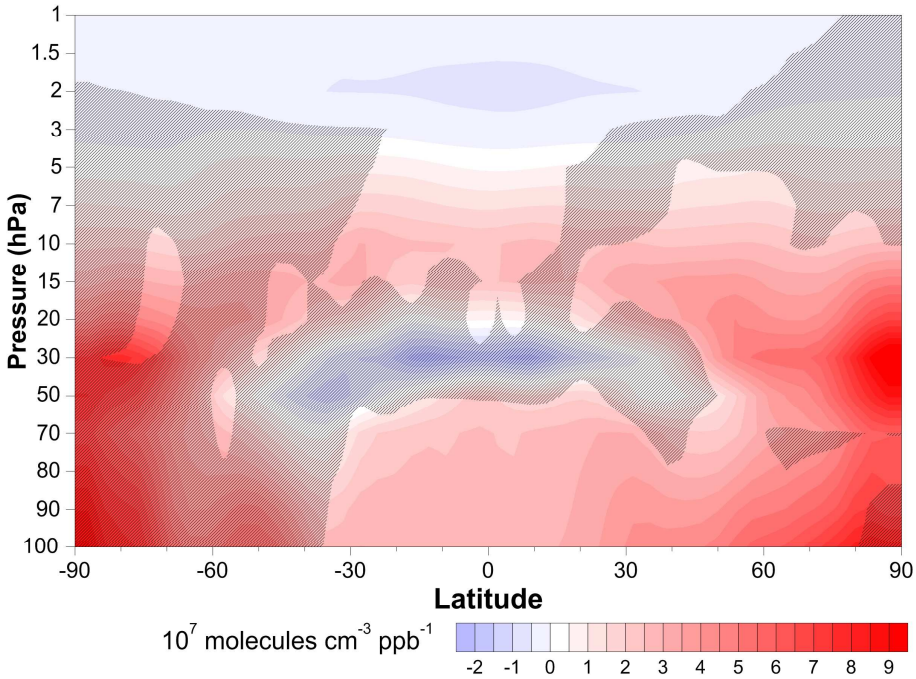

Fig. 9. Similar to Fig. 8, but the slopes are from simple linear regression models fitted to 2090s-mean ozone vs. 2090s-mean surface CH_4 for the four CH_4 simulations.

ACPD
12, 17583–17605, 2012